Fluctuations in the zeros of differentiable Gaussian processes

J. M. Smith, K. I. Hopcraft, and E. Jakeman
School of Mathematical Sciences, Applied Mathematics Division, University of Nottingham, NG7 2RD, United Kingdom
(Received 28 August 2007; revised manuscript received 4 December 2007; published 11 March 2008)

The stochastic point processes formed by the zero crossings or extremal points of differentiable, stationary Gaussian processes are studied as a function of their autocorrelation function. The properties of these point processes are mapped to the space formed by the parameters appearing in the autocorrelation function, their adopted form being sensitive to the structure of the autocorrelation function principally in the vicinity of the origin. The distribution for the number of zeros occurring in an asymptotically large interval are approximately negative-binomial or binomial depending upon whether the relative variance or Fano factor is greater or less than unity. The correlation properties of the zeros are such that they are repelled from each other or are "antibunched" if the autocorrelation function of the Gaussian process is characterized by a single scale size, but occur in clusters if more than one characteristic scale size is present. The intervals between zeros can be interpreted in terms of the autocorrelation function of the zeros themselves. When bunching occurs the interval density becomes bimodal, indicating the interval sizes within and between the clusters. The interevent periods are statistically dependent on one another with densities whose asymptotic behavior is governed by that of the autocorrelation function of the Gaussian process at large delay times. Poisson distributed fluctuations of the zeros occur only exceptionally but never form a Poisson process.

DOI: 10.1103/PhysRevE.77.031112 PACS number(s): 02.50.Fz, 05.45.Df, 89.75.−k

I. INTRODUCTION

Quantifying the properties of the zeros of a Gaussian process is of central importance to the topic of extremal statistics which impacts on numerous applications in biological [1–3], engineering [4–6], financial [7,8], and physical [9–12] sciences, in addition to seminal theoretical stimuli in pure probability [13,14] and practical developments in applied probability [15,16]. Consequently the subject has generated a large, diverse and technical literature across the years, which has been subject to three reviews [17–19]. Despite the topic's longevity, the generality that encompasses all its facets remains elusive, which is indicative of the problems' richness, inherent subtleties, and the individual demands of the diverse application areas. The essentials of the problem can be stated simply enough: Given a Gaussian process $x(t)$ with zero mean, variance σ^2, and autocorrelation function $\rho(\tau)=\langle x(0)x(\tau)\rangle/\sigma^2$, what are the statistical properties of the number of zeros that occur in an interval of length T, i.e., enumerating the instances and locations for when $x(t)=0$? The zeros are an example of the way in which a discrete, or point random process can be derived from an underlying continuous variation. This illustrates the relevance of the problem to the generation of, for example, pulselike phenomenology that can be manifested by complex systems (e.g. [20–22])—these being invariably nonlinear in character and containing a hierarchy of disparate time or length scales, and whose behaviors present significant challenges to model and interpret. Because the process to be considered is Gaussian, the multivariate joint statistics are prescribed in terms of the function ρ alone, and it is the properties of this function that influences principally the behaviors exhibited by and derived from the process. If the derivative of the process exists, then this is also Gaussian, hence the statistical properties of the zeros are also those of the turning points, which explains the relevance to extremal problems. Various ancillary problems attend the statistics of the zeros, for example the distribution of intervals between consecutive zeros or the "return probability"—which is a continuous random variable with stochastic process that is distinct from the underlying Gaussian process. Recent applications of this concept include, *inter alia*, characterizations of behaviors in sandpiles [23,24], finance [25], and networks [26]. The problem of enumerating zero crossings has a wider currency which continues to broaden, latterly being applied to the "nodal sets" of solutions to the Schrödinger equation, this being proposed as a method for classifying quantum chaos [27].

The seminal researches of Rice [28] and Kac [29] established, *inter alia*, that the integer number of zeros N occurring in an interval of length T has mean value $\langle N\rangle=\bar{r}T$, where $\bar{r}=[-\rho''(0)]^{1/2}/\pi$ is the rate. This expression shows immediately that for the mean to exist, the autocorrelation function must be twice differentiable at the origin, this condition being related to the smoothness of the trace of the process. Consequently, continuous and differentiable processes cannot have an autocorrelation function with a cusp singularity at the origin—if they do, they describe fractal processes, which are characterized by a hierarchical "inverse cascade" to progressively smaller scales where the number of zeros fails to be resolved by magnification. Rice's result stimulated an entire industry, whereby the conditions for its validity have been relaxed progressively, this being essayed in what is largely a highly technical literature [13,30,31], and latterly generalized to processes that are *functions* of a Gaussian process [32–35].

The fluctuations of the zeros have received considerably less attention. An investigation of the second factorial moment $\langle N(N-1)\rangle$ [4,36], showed that this quantity depends on the global values of ρ and its first and second derivatives in addition to those values at the origin. The expression for the second factorial moment can only be evaluated by quadrature, except for a special case [37], or for small values of T

as shown in Sec. II of this paper. Whilst formal expressions for the generalizations to higher order moments can be written down [31,38], these are of little practical value because of their complexity. This paper will, in part, give a detailed analysis of the second factorial moment of the zero crossings and its alternative formulation in terms of the Fano factor [39] as functions of the autocorrelation function of the Gaussian process, and it will be shown here that the fluctuations of the zeros are sensitive to the detailed structure of ρ near the origin and to a lesser extent its behavior for asymptotically large delay times.

The variation that is achievable in the second factorial moment prompts questioning what is the actual distribution for the number of zero crossings that occur in an interval, and it is the answer to this that forms the principal novelty of this paper. It will be shown from numerical realizations of Gaussian processes, that the distribution for the number of zeros that occur in an interval of size T are, in the limit of large values of T, approximately described by the binomial or negative binomial distributions depending upon whether the Fano factor is less or greater than unity, respectively. Only for the special case when the Fano factor is identically unity are the zeros approximately Poisson distributed. It is important to stress that the number of zero crossings is necessarily a *discrete* random variable and that properties of the stochastic process that is associated with the zeros do not have a continuum analogue. One such concept is antibunching and bunching, by which is meant the zero crossings are respectively repelled or attracted to one-another. This notion follows from an analysis of the autocorrelation function for the zeros themselves and the probability density function of the times between successive crossings—the interevent time. Both of these quantities are influenced principally by the structure of the autocorrelation function of the Gaussian process near the origin.

Interevent time is a residue of the zero or level crossings of a process, and is closely related to the concept of "persistence" which measures the time that a process is above a prescribed threshold (e.g. [9–12]). The general literature associated with the generic properties of interevent times is also mature (e.g. [18]), with few analytical results. A notable exception is the result obtained in [40], which is particular for the autocorrelation function having the specific form

$$\rho(\tau) = \frac{3}{2}\exp\left(\frac{-|\tau|}{\sqrt{3}}\right)\left[1 - \frac{1}{3}\exp\left(\frac{-2|\tau|}{\sqrt{3}}\right)\right] \tag{1}$$

that is exponentially bounded. This process has an interevent time density function expressible in terms of elliptic integrals that is unimodal, peaking at zero and having an exponential tail. This analytical result serves as one of the benchmarks used for validating the numerical methods to be employed in this paper. Interevent times were investigated for processes with autocorrelation function having a power-law asymptote [41,42]. It was found that the asymptotic form of the density of interevent intervals depended on the power-law index γ, being exponential when $\gamma \geq 1$ and a stretched exponential when $0 < \gamma < 1$, the degree of stretching being the index. This result is in accord with earlier theoretical work on the slightly different problem for the asymptotic behavior for their being *no* crossings in the interval [43]. However, it is a consideration for the process of the zero crossings themselves that comprises the principal theme of this paper, the interval distributions being subsidiary to this problem.

This paper will explore the sensitivity of the zero-crossing process to the smoothness properties and scale sizes associated with the underlying Gaussian process that generates them. The contents of the paper are organized as follows. Section II evaluates the second factorial moment of the zeros for three autocorrelation models and discusses why the Fano factor is a more sensitive and appropriate measure to use for gauging their fluctuations. The parameters appearing in the autocorrelation functions create a landscape in which the properties of the zeros change and can be classified. Section III presents the results of simulations of Gaussian processes formed with three model autocorrelation functions from which are obtained the point processes of the zeros. The measures used to characterize these are the probability distribution of the zeros themselves, their autocorrelation function and the probability density for the interevent intervals. The characterization of different types of behavior is identified with specific regions of the parameter space introduced in Sec. II. A summary and discussion forms the concluding Sec. IV. Technical details concerning the power spectra associated with the Gaussian processes are assigned to the Appendix.

II. CHARACTERIZATION OF PROCESSES BY THEIR SECOND MOMENT

This section evaluates the second factorial moment of the number of zero crossings of a Gaussian random process occurring in an interval of size T as a means to gauge of their fluctuations. These fluctuations are sensitive to the form adopted by the autocorrelation function of the Gaussian process and this susceptibility will be explored through invoking three autocorrelation models that possess different smoothness, scale-size, and correlation-memory properties. The second factorial moment was first derived in [36] and was subsequently rewritten in a more usable form by Middleton [4] as

$$\langle N(N-1)\rangle = \frac{2T^2}{\pi^2}\int_0^1 (1-y)\frac{|A^2 - B^2|^{1/2}}{(1-\rho^2)^{3/2}} \times \left[1 + \frac{B}{|A^2 - B^2|^{1/2}}\arctan\left(\frac{B}{|A^2 - B^2|^{1/2}}\right)\right] dy, \tag{2}$$

where

$$A = -\rho''(0)[1 - \rho^2(yT)] - \rho'^2(yT),$$

$$B = \rho''(yT)[1 - \rho^2(yT)] + \rho(yT)\rho'^2(yT),$$

with ρ the autocorrelation function and the prime representing differentiation with respect to its argument. It is not usually possible to evaluate Eq. (2) analytically, although this was achieved by Miroshin [37] for the same autocorrelation

function Eq. (1) employed by Wong [40] to yield a numerical value of $\langle N(N-1)\rangle \approx 0.1287$. We are able to reduce considerably the complexity of Eq. (2) in the small T limit. Consider a "subfractal" [44,45] autocorrelation function with expansion near the origin given by

$$\rho(\tau) = 1 - \frac{(\pi\bar{r})^2}{2}\tau^2 + b|\tau|^{2+\mu} + \cdots, \quad 0 < \mu < 2, \tag{3}$$

where $\bar{r}$ is the mean zero rate, given by Rice [28], and b and μ are parameters that allow the behavior of the autocorrelation function to be manipulated. Substitution of Eq. (3) into Eq. (2) and expanding about $T=0$ yields

$$\langle N(N-1)\rangle \approx \left[\frac{(4-\mu^2)^{1/2}}{\mu} + \arctan\left(\frac{\mu}{(4-\mu^2)^{1/2}}\right)\right] \times \frac{2|b|}{\pi^3\bar{r}}T^{1+\mu} + O(T^{1+2\mu}). \tag{4}$$

The *normalized* second factorial moment

$$N^{[2]} = \frac{\langle N(N-1)\rangle}{\langle N\rangle^2}.$$

therefore scales as $T^{\mu-1}$. Note that, if $\mu=1$, then $N^{[2]}$ is independent of T [44].

Although this analysis is only valid for values of $T \ll 1$, it does show that it is possible to characterize some behavior of the zeros in terms of the parameters appearing in the autocorrelation function in a closed form. Whilst the scaling of the second moment for small values of T is interesting, it is desirable to investigate how the fluctuations behave for larger values of T. This is because the second factorial moment is defined by an integral, which is indicative of a global dependence on T. A cursory inspection of Eq. (2) shows that the form of $\langle N(N-1)\rangle$ for $T \gg 1$ is dominated by the T^2 prefactor, indeed in this limit

$$\langle N(N-1)\rangle \sim \frac{2T^2}{\pi^2}\int_0^1 (1-y)|-\rho''(0)|dy + O(T) = (\bar{r}T)^2 + O(T)$$

and so

$$\langle N(N-1)\rangle \sim \bar{r}^2T^2 + YT + Z,$$

where Y and Z are functions of the autocorrelation function and its derivatives, whose values are embedded in the integral expression (2). Consequently, the normalized second factorial moment tends to unity in the limit of large T. This can be contrasted with the behavior of the Fano factor [39], or variance of the zeros relative to their mean, defined by

$$F(T) = \frac{\langle N^2\rangle - \langle N\rangle^2}{\langle N\rangle} = \frac{\langle N(N-1)\rangle}{\langle N\rangle} - \langle N\rangle + 1,$$

from which it can be seen that

$$F(T) \sim \frac{Y}{\bar{r}} + 1 \tag{5}$$

when $T \gg 1$. The Fano factor can be considered to be a measure of how *Poissonian* are the number fluctuations, for when $F=1$ the variance equals the mean, which is characteristic of Poisson statistics. A comprehensive discussion of the use of the F for characterizing discrete fluctuation phenomena can be found in [46]. The distribution of the zeros can be said to be super-Poissonian when $F>1$ or sub-Poissonian when $F<1$. It evidently follows from Eq. (5) that the Fano factor tends to a limit that is unity only when $Y \equiv 0$. Thus the Fano factor is a more sensitive discriminator of the fluctuations of the zeros than is the normalized second factorial moment.

To explore the effects that changes in the autocorrelation function ρ have on both the value of F and the behavior of the zeros, we consider three models. The first of these is a modification to the exponentially bounded Gaussian autocorrelation function:

$$\rho_1(\tau) = \left[1 + b\left(\frac{|\tau|}{L}\right)^{2+\mu}\right]\exp\left(-\frac{|\tau|^2}{2L^2}\right), \tag{6}$$

where b and μ are parameters and L is the correlation length. Note that Eq. (6) contains two intrinsic scale sizes, the first characterizing the exponential cutoff $l_1 \sim L$ and the second $l_2 \sim L/|b|^{1/(2+\mu)}$ associated with the prefactor, whose value can be greater or less than L depending upon the size of b and μ. However, b and μ are not entirely arbitrary because $\rho(\tau)$ must decrease away from the origin and $|\rho(\tau)| < 1$ other than at the origin [47]. All values of b and μ that are discussed subsequently are selected to conform to these constraints. Furthermore, the power spectrum must be a positive definite quantity and this is the case if $b \geq 0$; therefore, this model, and the others to be considered, cannot treat anticorrelated processes (see the Appendix). The parameter $\mu > 0$ affects the smoothness of the trace of any realization as can be seen from the expansion of (6) close to the origin

$$\rho_1(\tau) \approx 1 - \frac{1}{2}\left(\frac{|\tau|}{L}\right)^2 + b\left(\frac{|\tau|}{L}\right)^{2+\mu} + \frac{1}{4}\left(\frac{|\tau|}{L}\right)^4 + \cdots, \tag{7}$$

so that $\bar{r} = 1/(\pi L)$. Note that the fourth derivative at the origin is singular when $0 < \mu < 2$ corresponding to any trace formed from a realization of the process having a derivative that is continuous but not differentiable. For this reason the model (6) is referred to as being "subfractal". If $b \equiv 0$ then ρ_1 has a single scale and is infinitely differentiable corresponding to a smooth process.

Using Eq. (6) in Eq. (2) enables a range of processes with different Fano factors to be determined in the limit $T \gg L$ as μ and b are changed, resulting in the contour plot shown in Fig. 1(a). The contour for which $F(\infty)=1$ is highlighted on the figure and evidently a range of sub- and super-Poissonian behaviors is achievable. The line $b=0$ corresponds to the purely Gaussian autocorrelation function with $F(\infty) \approx 0.57$. If the second characteristic scale size becomes smaller than L, then traces formed by realizations of the process become more crenellated. A cluster of zeros will occur if, on average, there are two or more zeros in a characteristic length, and this happens if $l_2 \equiv L/|b|^{1/(2+\mu)} \lesssim 2L$, i.e., if $|b| \gtrsim 1/2^{(2+\mu)}$, and the locus of this curve is shown by the dotted lines on Figs. 1(a) and 1(b). Below the line only a single scale occurs

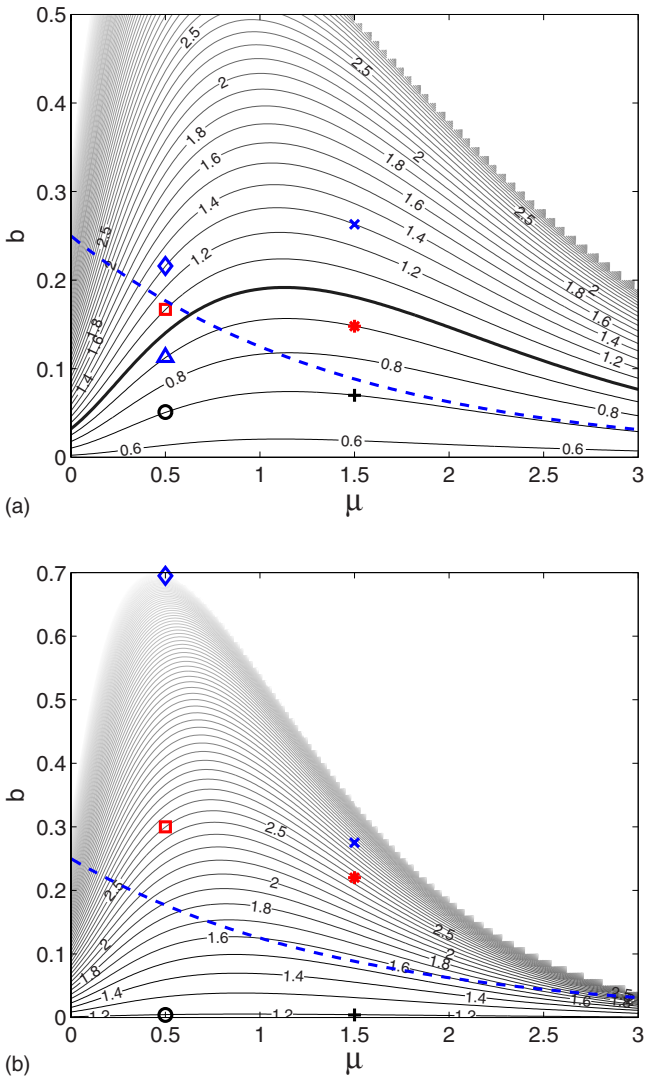

FIG. 1. (Color online) Contour plot of the Fano factor of the zeros of the Gaussian process. The plot shows $F(10000L)$, which approximates $F(\infty)$, as a function of b and μ, which parametrize the autocorrelation function given by (a) Eq. (6) and (b) Eq. (8). The thicker contour corresponds to $F(\infty)=1$, and the colored symbols denote the values used in subsequent simulations. The dotted line marks where $|b|=1/2^{(2+\mu)}$; above this line two scales are present; below the line only a single scale.

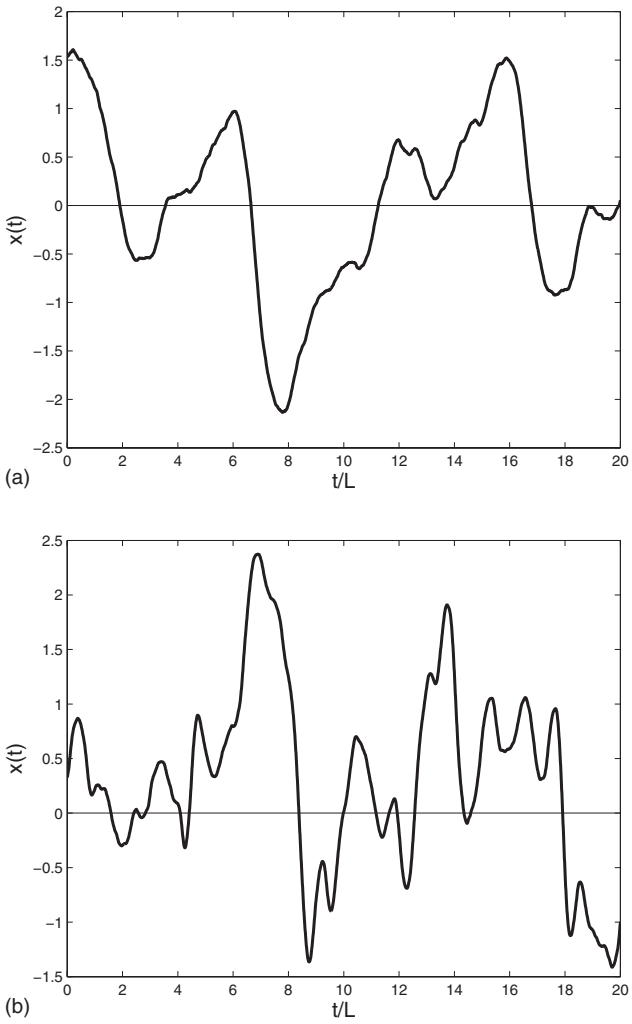

FIG. 2. Fragments of realizations of $x(t)$ having the same mean and Fano factor $F=0.9$ for the number of zero crossings but with (a) $\mu=0.5$ and (b) $\mu=1.5$. The additional scale size is clearly evident in (b). The units of the $x(t)$ axis are arbitrary but identical in both realizations.

in a correlation length; above the line there is an additional characteristic scale size. This is exemplified by the two realizations of the stochastic process that are shown in Fig. 2 which correspond to points in Fig. 1(a) that lie on the same contour $F=0.9$ but on either side of the two-scale line, and are denoted on the figure by the triangle and the asterisk. These realizations therefore have identical values for the mean value of the zero crossings and for their Fano factor $F=0.9$ but that shown in Fig. 2(a) has a single scale size associated with it, whereas Fig. 2(b) has two scales, which results in its more undulating appearance. Note however that although the trace shown in Fig. 2(b) has more random "oscillations", the *slope* of the trace shown in Fig. 2(a) is more erratic. This realization corresponds to a smaller value of μ which therefore has more pronounced subfractal characteristics, which we shall describe subsequently as "jitter".

The second model is a modification of LCR noise [4] that has a similar parametrization as the model for ρ_1,

$$\rho_2(\tau)=\left[1+\frac{|\tau|}{L}+b\left(\frac{|\tau|}{L}\right)^{2+\mu}\right]\exp\left(-\frac{|\tau|}{L}\right) \tag{8}$$

but is characterized by a longer correlation "memory" by virtue of the exponential rather than the Gaussian tail. The role of μ and b is as before: To establish an additional scale size and to imbue subfractal characteristics for when $0<\mu<2$. The expansion of this model for small delay times always contains a cubic term:

$$\rho_2(\tau)\approx 1-\frac{1}{2}\left(\frac{|\tau|}{L}\right)^2+b\left(\frac{|\tau|}{L}\right)^{2+\mu}+\frac{1}{3}\left(\frac{|\tau|}{L}\right)^3+\cdots, \tag{9}$$

and this is identical with Eq. (7) up to order $\tau^{2+\mu}$ if $0<\mu<1$. The map of the Fano factor is calculated using Eq. (2)

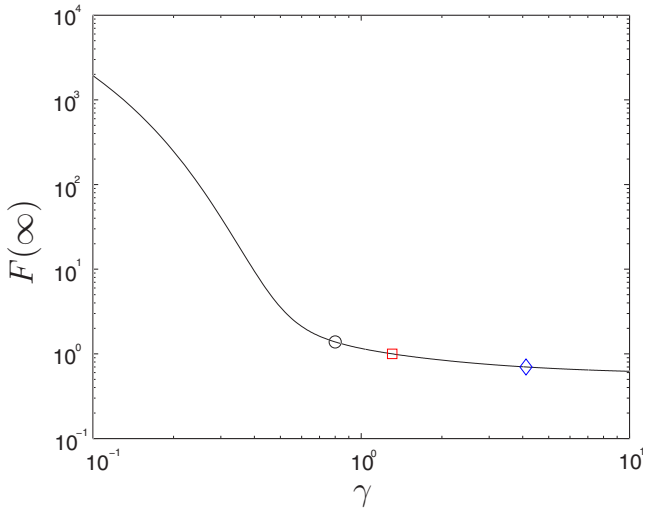

FIG. 3. (Color online). Plot of the Fano factor of the zeros of the Gaussian process correlated with ρ_3. The plot shows $F(100000L)$, which approximates $F(\infty)$, as a function of the index γ. The symbols correspond to the values of γ used in the simulations.

and shown in Fig. 1(b). Notice that the Fano factor is always greater than unity principally because of the longer correlation memory associated with this model. The symbols on the figure refer to values used in subsequent simulations.

The final model for the autocorrelation function that will be considered has a much longer decay than the Gaussian and LCR models. Recent work [41,42] has examined the asymptotics of interevent density functions for the zeros of a Gaussian and non-Gaussian processes with autocorrelation function having a power-law asymptote. The model we adopt has the form

$$\rho_3(\tau) = \left[1 + \frac{1}{\gamma}\left(\frac{\tau}{L}\right)^2\right]^{-\gamma/2}, \tag{10}$$

whose expansion about the origin is

$$\rho_3(\tau) \approx 1 - \frac{\tau^2}{2L^2} + \left(\frac{1}{8} + \frac{1}{4\gamma}\right)\frac{\tau^4}{L^4} + \cdots,$$

but with asymptote $\sim\tau^{-\gamma}$. A key difference between this model and the others considered in this paper is that it is smooth to all orders and has a well defined single characteristic scale size despite the power-law asymptote. This is because there is an inner scale, as revealed by the factor "1" in Eq. (10), which ensures that the zeros have well-defined moments whose values are not dependent upon resolution size. Note that, as $\gamma\to\infty$, $\rho_3(\tau)\to\exp(-\tau^2/2L^2)$, which is model (6) with $b=0$.

Figure 3 shows $F(\infty)$ on log-log axes as a function of γ, which can be less or greater than unity and is monotonically decreasing with increasing γ. The symbols correspond to the values of γ used in the subsequent simulations. Note that a range of values of $F(\infty)$ can be achieved by slight variations in the index when $\gamma<1$. Note that $F(\infty)=1$ when $\gamma\approx1.31$. For $\gamma\gg1$, the value of $F(\infty)$ tends to the Gaussian value of 0.57, as expected from the form of Eq. (10) in this limit.

The Fano factor gives an indication of the fluctuations of the zeros but does not indicate how they evolve as a process. To achieve this objective requires simulating the process since no analytical results of sufficient generality exist. This is carried out in Sec. III.

III. SIMULATION RESULTS

Gaussian random processes may be simulated by convolving Gaussian random numbers with a prescribed autocorrelation function. The convolution can be performed directly or by a spectral technique [48] and the latter method enables fast Fourier transforms (FFT) to be deployed to advantage, thereby decreasing significantly the number of operations required. For a realization of length M, the direct method needs $\sim M^2$ calculations compared with $\sim M\log M$ for the spectral method. The direct method is particularly expensive to use for power-law correlation functions. The direct and spectral methods can always be employed on allowable autocorrelation functions, i.e., those with positive power spectra. Extreme care must be exercised when using nonstandard autocorrelation functions such as those given by Eqs. (6) and (8), because both these violate this condition when b is negative. Further discussion on this matter can be found in [49] and the Appendix.

For the Gaussian and LCR models we formed 500 000 independent realizations each of length 100 000 unit intervals; this is an adequate length because of the exponential outer scale of the autocorrelation functions, which was taken to be $L=100$. The zeros of the processes are located and the resulting statistics, when averaged over all realizations, have been verified by comparison with the few known analytical results, comprising the mean $\langle N\rangle$ from Rice [28], the second factorial moment $\langle N(N-1)\rangle$ from Steinberg [36], and an interval distribution from Wong [40]. The correlation length can be interpreted as the resolution of the process: increasing it allows the process to be resolved in more detail but would require more points in order to see the same number of events; for example, the number of zeros. It follows that the number of zeros in a time T is inversely proportional to L, as verified by Rice's formula. For each realization, the following quantities were determined from the data.

(1) The discrete distribution of the zeros occurring in an interval of length $T=1000L$, which is sufficiently long for moments of the distribution to approximate adequately the theoretical values of $F(\infty)$ given in the contour plots.

(2) The continuous probability density function $q(\Lambda)$ for the intervals between consecutive zeros, $q(\Lambda)d\Lambda$ being the probability of finding an interval in the range Λ to $\Lambda+d\Lambda$.

(3) The autocorrelation function of the zeros themselves.

The simulations are performed in discrete time with a temporal resolution $\delta t=1$ and with L chosen to be sufficiently large so as to ensure that there is at most one zero in the interval δt so that all zero crossings are counted. Values of L in the range $10\le L\le100$ are sufficient to achieve this; the lower value being appropriate for the completely smooth process defined by ρ_3, the upper value being suitable for the subfractal models. The autocorrelation function of the zeros is formed from an ensemble average over K realizations of

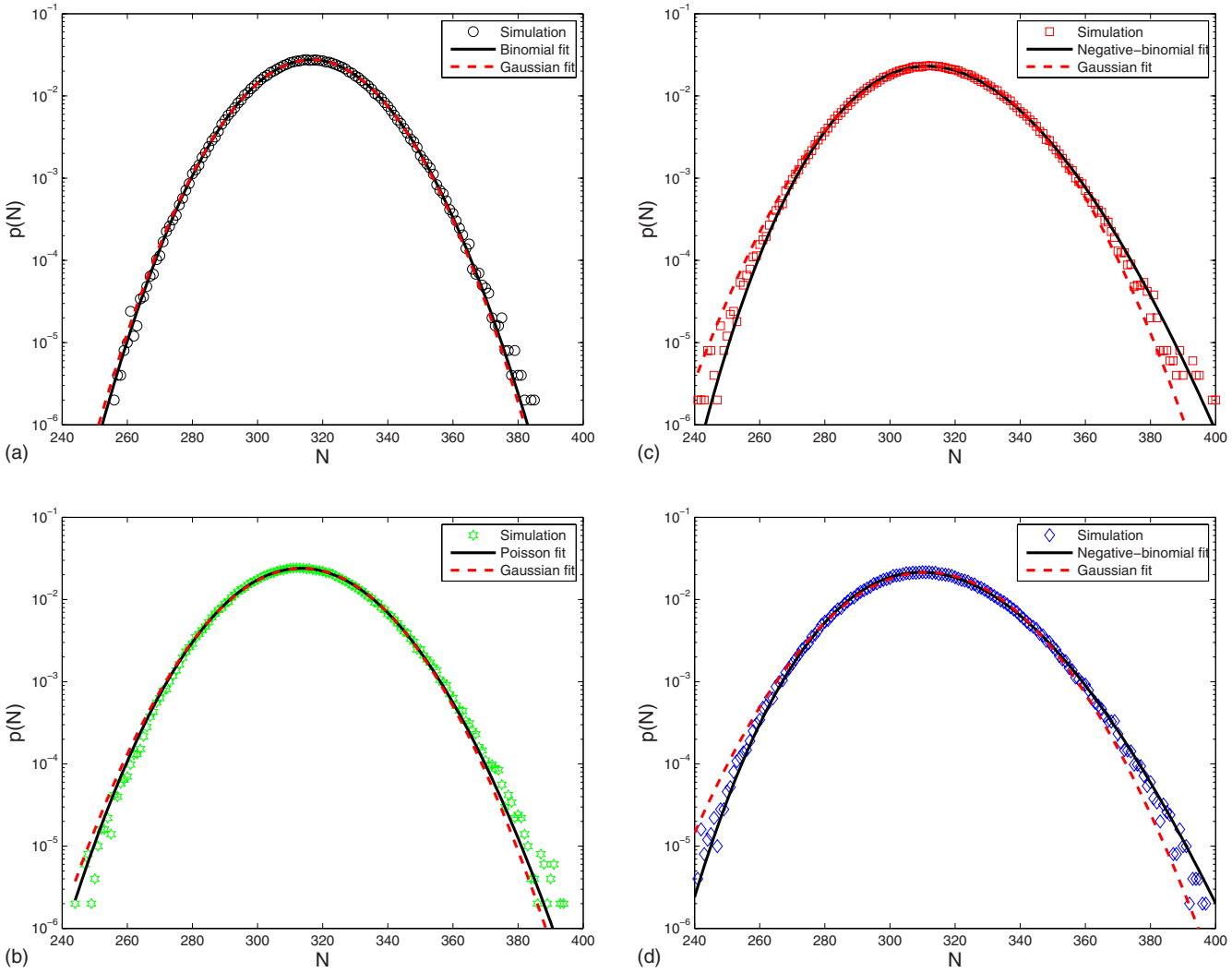

FIG. 4. (Color online) Probability distributions $p(N)$ for the number of zero crossings of a Gaussian process generated with autocorrelation model ρ_1 occurring in an interval of length $T=1000L$. The parameter μ is fixed at 0.5 with (a) $b=0.051$, (b) $b=0.140$, (c) $b=0.167$, and (d) $b=0.216$, which correspond to $F(\infty)=0.7$, $F(\infty)=1$, $F(\infty)=1.1$, and $F(\infty)=1.3$, respectively. The solid line shows a fit with (a) the binomial distribution, (b) the Poisson distribution, and (c) and (d) the negative-binomial distribution; the dotted line in each figure is the Gaussian density function with the same mean and variance. All figures are simulated with $L=100$ and averaged over 500 000 realizations.

the process. The values of K required to achieve convergence with the theoretical values of the Fano factor obtained from Eq. (2) are 50 000 for ρ_1 and ρ_2, and 1.5×10^6 for ρ_3. Let $N_k[\Delta(t)]$ denote the number of zeros from the kth realization of the process that occurs in an interval $\Delta(t)$that is located at $t=m\delta t$ along the time axis. The autocorrelation function of the zeros $\langle N(t)N(t+\tau)\rangle \equiv C(\tau)$ is determined from

$$C(\tau) = \lim_{K\to\infty} \frac{1}{KM} \sum_{k=1}^{K} \sum_{m=1}^{M} N_k[\Delta(m\delta t)] N_k[\Delta(m\delta t + \tau)].$$

Note that as the separation time τ becomes larger than the characteristic fluctuation time of the process, the number of zeros in the intervals become independent of each other and so

$$C(\tau) = \bar{r}^2,$$

where $\bar{r}=1/\pi L$ is the mean number of zeros in a resolution interval δt. The normalized autocorrelation function is

$$C^{[2]}(\tau) = \frac{C(\tau)}{\bar{r}^2},$$

and has the property that $C^{[2]}\to 1$ for $\tau \gg 1$. When $C^{[2]}<1$ the zeros are antibunched, or repelled from each other, whereas when $C^{[2]}>1$ the zeros are bunched or clustered. In all subsequent figures featuring $C^{[2]}(\tau)$ and $q(\Lambda)$, the delay time τ and random variable Λ are measured in units of the correlation length L.

A. Modified Gaussian model

Figures 4(a)–4(d) shows the probability distribution for the number of zeros for a selection of μ-b pairs that are

located in different parts of the map of Fig. 1(a). The symbols used in Fig. 4 are replicated by the points in Fig. 1(a). When $F<1$, the distribution for the number of zeros occurring in the interval T is approximately binomial, which when parametrized in terms of F and $\langle N\rangle$ has the form

$$p_b(N) = \frac{\alpha!}{N!\,(\alpha-N)!}F^{\alpha-N}(1-F)^N,$$

where $\alpha=\langle N\rangle/(1-F)$ and this theoretical model fit is shown by the full curve in Fig. 4(a). Also shown by the dotted line for comparison is the Gaussian density function with the same mean and variance, although it should be borne in mind the number of zero crossings is a *discrete* quantity and so only discrete probability distributions are appropriate descriptors of their fluctuations. A simple interpretation for F in this instance is that it represents the probability of obtaining a zero in an interval of length $\sim\alpha\delta t$. If $F>1$, the distribution of the zeros can be approximated by the negative binomial distribution, which when written in terms of F given by

$$p_n(N) = \frac{(\alpha-1+N)!}{N!\,(\alpha-1)!}F^{-\alpha}\left(1-\frac{1}{F}\right)^N,$$

where now $\alpha=\langle N\rangle/(F-1)$and this theoretical model fit is shown by the full curves in Figs. 4(c) and 4(d), where again the Gaussian density is shown by the dotted line for comparison. Here it can be seen that the Gaussian distribution is less accurate than the negative-binomial model in the extreme tails, and fails to capture the skewness of the distribution. When $F=1$, the distribution of the zeros can be approximated by the Poisson distribution,

$$p_p(N) = \frac{\langle N\rangle^N}{N!}\exp(-\langle N\rangle),$$

and this model fit is shown by the full curves in Fig. 4(b). The Poisson can be obtained as the unique discrete limiting distribution of the binomial or negative-binomial distributions as $F\to 1$.

A common "figure of merit" for determining how closely a model distribution matches data is the chi-squared measure,

$$\chi^2 = \sum_{N=1}^{m}\frac{[f_N-p(N)]^2}{p(N)}, \tag{11}$$

where f_N are the measured frequencies of obtaining N zeros and $p(N)$ are the expected frequencies according to the chosen model distribution. When Eq. (11) is used to assess the goodness of fits of the binomial, negative binomial, Poisson and Gaussian distributions, denoted χ_b^2, χ_n^2, χ_p^2, and χ_g^2, respectively, we find that when $F=0.7$ (the black markers), then $\chi_b^2\approx 200$, $\chi_p^2\approx 1.2\times 10^3$, and $\chi_g^2\approx 310$. This shows that the binomial distribution is the closest to the data of the three. When $F=1.1$ (denoted by the red markers), then $\chi_n^2\approx 410$, $\chi_p^2\approx 740$, and $\chi_g^2\approx 1.25\times 10^3$, and for $F=1.3$ (denoted by the blue markers), then $\chi_n^2\approx 200$, $\chi_p^2\approx 900$, and $\chi_g^2\approx 1.56\times 10^3$, so that the negative binomial distribution is the best fit for when $F>1$. When $F=1$, however, χ_b^2, χ_n^2, and χ_p^2 all result in $\chi^2\approx 500$, indicating that the Poisson distribution is the most appropriate fit; the corresponding value for the Gaussian fit is $\chi_g^2\approx 1.25\times 10^3$. Figures 5(a) and 5(b) shows $C^{[2]}(\tau)$ for the same points that were featured in the foregoing discussion together with the interevent probability densities shown in Figs. 5(c) and 5(d). Consider together Figs. 5(a) and 5(c), which are for $\mu=1/2$ and b increasing from the sub- to the super-Poissonian region whilst simultaneously traversing the curve between one and two scales. The point $b=0.051$, denoted by circles, occurs in the single-scale sub-Poissonian region with $F<1$, and $b<2^{2+\mu}$. The autocorrelation is largely <1 (denoting anticorrelation), with a shallow and broad maximum located at $\tau\sim 2L$. Any correlation is weak beyond $\tau\sim 5L$. The interevent density corresponding to this is unimodal, the location of the peak coinciding approximately with the maximum in the correlation function. This peak is indicative of the mean spacing between the zeros, which in this case are isolated from each other. The tail of the density is exponential—a feature common to all examples using this model. The value $b=0.167$, denoted by squares in the figures, occurs in the super-Poissonian region but is located in the proximity of the two-scale boundary curve. The correlation function is greater than unity for small delay times, falling below one for $0.5\lesssim\tau/L\lesssim 2.5$ and becoming essentially uncorrelated thereafter. The corresponding interevent time density remains unimodal but has filled toward the origin, which is symptomatic of a wider range of shorter-valued interevents being present. Hence the zeros have less of a tendency to be isolated from each other, there being an incipient trend toward clustering. The point $b=0.216$ is denoted by the diamond-shaped symbol and also occurs in the super-Poissonian region but is located in the two-scale region where $b>2^{2+\mu}$. The values for τ where the correlation function is greater than unity has broadened out from the origin, and the region where it is less than one narrowed. The interevent density has evolved into a bimodal function, the peak closest to the origin corresponding to intervals within a cluster of zeros and the second peak representing the interval between clusters. The intracluster peak is a maximum at the origin indicating that zeros can occur in close proximity to each other. This trend toward shorter intervals within a cluster is a consequence of the Gaussian process being affected by the subfractal jitter in this region in of the μ-b plane. Another indicator of this smoothness property is that all the autocorrelation functions decrease away from the origin irrespective of whether they are positively or anticorrelated. Contrasting all the densities in Fig. 5(c), note that second peak occurs at progressively larger values of Λ/L, indicating that as F increases the clusters of zeros are moving further apart, whilst the intervals between zeros within a cluster get progressively shorter. Figures 5(b) and 5(d) reveal a complementary picture, but one which differs subtly in detail due to the processes being in a region of μ-b space that correspond to smoother realizations. All of these results are for $\mu=1.5$ with the two-scale region being crossed as b increases. The unaltered features are the existence of a unimodal interevent density coupled with a single peaked autocorrelation in the single scale region corresponding to $b=0.07$ as shown by the crosses, and bimodal densities with double-peaked autocorrelation functions in the two-scale region for the two other examples. Where the re-

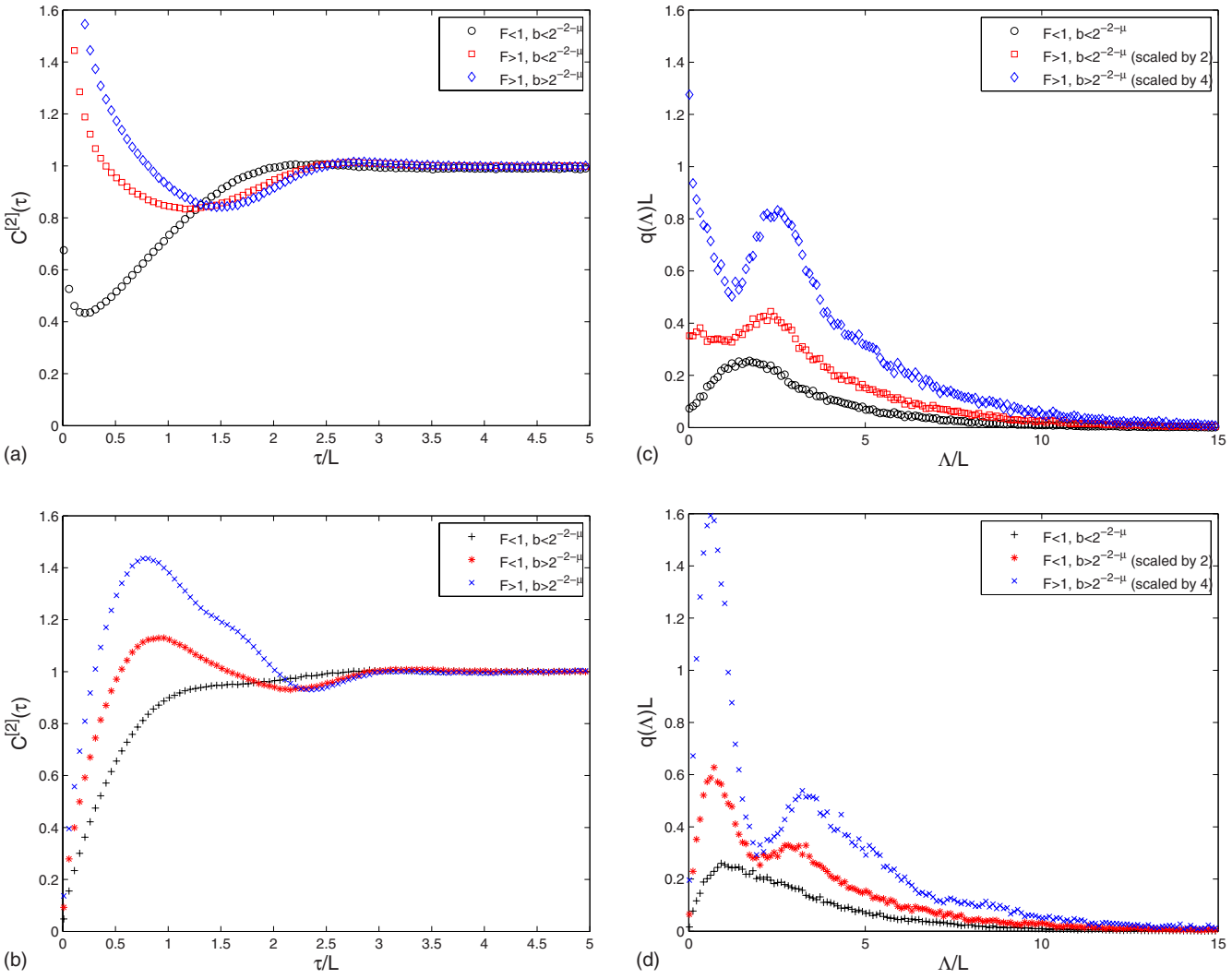

FIG. 5. (Color online) (a) Normalized autocorrelation function $C^{[2]}$ of the zeros of Gaussian processes correlated with ρ_1 and $\mu=0.5$, plotted as a function of the delay time in correlation lengths τ/L. The circles, squares, and diamonds correspond to values of b equal to 0.051, 0.167, and 0.216, respectively. In (b), the value of $\mu=1.5$ and the plus signs, stars, and crosses correspond to values of b equal to 0.070, 0.148, and 0.263, respectively. In (c) and (d), the normalized interevent densities of the zeros of the Gaussian process are shown, where the symbols correspond to the same values of b as featured in (a). The densities have been scaled so that they may be distinguished. All figures are simulated with $L=100$ and averaged over 500 000 realizations.

sults differ is that all the autocorrelation functions now increase away from the origin and that the first peak of the interevent densities is displaced from the origin indicating the intervals within a cluster have themselves become separated. In all these results the principal features of the correlation function and interevent densities occur at the similar values of delay time or interval when both measured in units of L. Hence the zeros are essentially never statistically independent of each other except at large delay times. It is worth stressing that on the contours $F=1$, although the distribution of the zeros is described by the Poisson distribution, they do not form a Poisson process which requires independent intervals with exponential distribution. As the $F=1$ contour is followed, the process moves through various regimes as μ increases. First a single-scale regime whose value is characteristic of the distance between the zeros but the subfractal "jitter" is of insufficient magnitude to bring the zeros closer together. This passes into a two-scale region, where a tendency emerges for the zeros to cluster together, each cluster becoming separated from the next. This is succeeded by a smoother two-scale region where the zeros form clusters, but the zeros are well separated within each cluster.

B. Modified LCR model

Processes were also simulated using Eq. (8) as a model for the autocorrelation function. The principal similarity is that the zeros are well approximated by the negative binomial distribution [$F(\infty)>1$ for this model]. Figure 6 shows the resultant inter event densities of the zeros for a selection of points in the μ-b plane. These results exhibit the same characteristics as seen for the previous model but the individual features are less prominent. This is because they are dominated by the subfractal jitter caused (at least) by the

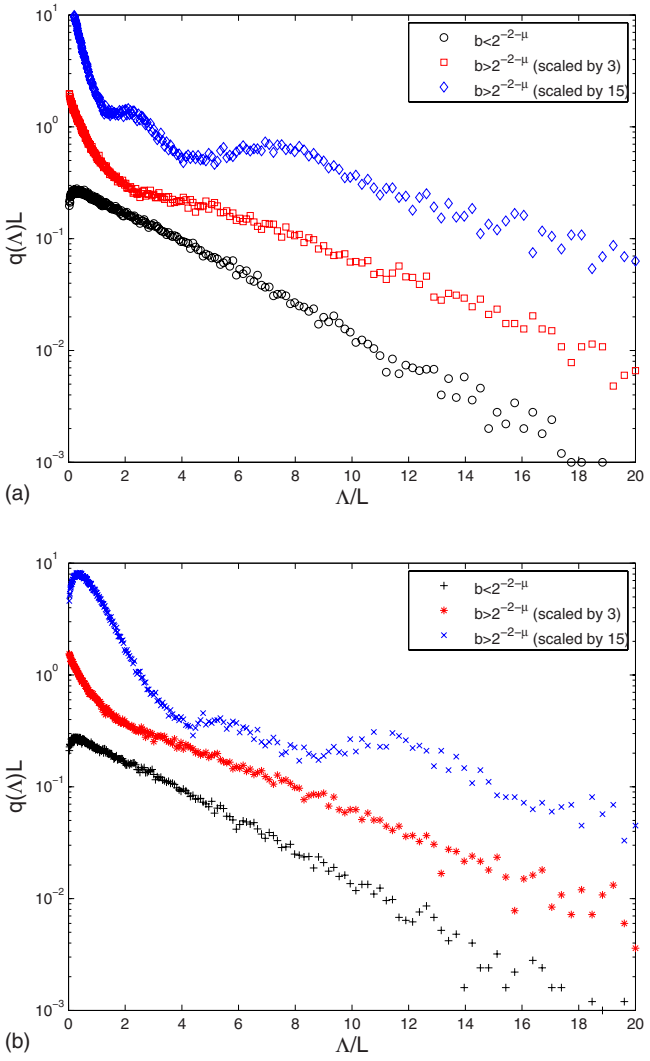

FIG. 6. (Color online) Normalized interevent density functions of the zeros of Gaussian processes correlated with ρ_2, plotted as a function of the delay time in correlation lengths τ/L. In (a), $\mu=0.5$ and the circles, squares, and diamonds correspond to values of b equal to 0.004, 0.300, and 0.695, respectively. In (b), $\mu=1.5$ and the plus signs, stars, and crosses correspond to values of b equal to 0.004, 0.220, and 0.275, respectively. All figures are simulated with $L=100$ and averaged over 500 000 realizations.

always present cubic term in the autocorrelation function, whose effect has a more persistent memory by virtue of the exponential rather than Gaussian tail. In Fig. 6(a), $\mu=0.5$ and the circles, squares, and diamonds correspond to values of b equal to 0.004 $[F(\infty)=1.2]$, 0.300 $[F(\infty)=2.5]$, and 0.695 $[F(\infty)=8.6]$, respectively. The selected values of b fall on either side of the two-scale boundary curve. The density function for the smallest value of b is similar in form to the equivalent case shown in Fig. 5(c), being unimodal with peak value displaced very slightly from the axis after which the exponential tail becomes established. Significantly, the density function does not fall to zero at the origin, so there are a range of small interval sizes within the scale characterizing the modal value, this being an indication of the most likely spacing between the zeros. The intermediate value of b is located ostensibly in the two scale region, though this is not particularly evident from a first inspection of the density function. This function is unimodal with peak on the axis, having a sharp decline over two correlation lengths, followed by a plateau of width $4L$ and then an exponential tail, but with different characteristic scale size compared with that near the origin. Hence there are two distinct scale sizes that characterize the behavior. The zeros therefore do fall into a hierarchy of clusters, but it is substantially influenced by the strong subfractal effect that causes erratic changes in the direction of a realization rather than changes in its value. The last value of b is selected to illustrate that density function does eventually become bimodal, the first peak being on axis and the second occurring at $2L$. The correlation functions for the zeros are not shown because their interesting features reflect essentially the same information, as was seen in Figs. 5(a)–5(c).

In Fig. 6(b), $\mu=1.5$ and the plus signs, stars, and crosses correspond to values of b equal to 0.004 $[F(\infty)=1.2]$, 0.220 $[F(\infty)=2.5]$, and 0.275 $[F(\infty)=3.3]$, respectively. These points occur in the region of the μ-b plane corresponding to smoother realizations than those shown in Fig. 5(a), but which are rougher than those shown in Fig. 6(d). The form of the density functions for the smallest and intermediate values of b are very similar to the equivalent plots in Fig. 5(d). The final plot shows the first semblance of a bimodal distribution where, significantly, the first peak is now displaced from the axis, as was the case in Fig. 5(d).

C. Power-law model

This model given by Eq. (10) requires significantly longer and more (1.5×10^6) realizations to achieve the required accuracy for the mean and Fano factor. It is fortunate that the Fourier method can be used for this model since performing such long and so many realizations by the direct method would prove to be computationally onerous. It is important to ensure that the autocorrelation function decays sufficiently close to zero over the realization length. When $\gamma>1$ $(F<1)$ it is found that realizations of length 10^4L with a value $L=10$ is sufficient but that this must be increased to 10^5L when $\gamma=0.8$ $(F>1)$. As before, the distribution of the zeros is negative binomial, Poisson, or binomial, according to whether the Fano factor exceeds $(\gamma=0.8)$, equals $(\gamma=1.305)$, or is less than unity $(\gamma=4.113)$. Figure 7 shows the autocorrelation functions and inter event densities for these three examples which accord with the smooth, single-scale behaviors as described in the discussion that accompanies Figs. 5(b) and 5(d). Where they differ is in the asymptotic behavior of the correlation function and interevent densities. There is residual correlation at long delay times; the tail of the interevent density is a stretched exponential $\exp(-\Lambda^\gamma)$ when $\gamma\leq1$, as reported elsewhere [41,42]. Thus the long memory effects that characterize the Gaussian process become manifested in the attendant correlation behavior of the zeros.

IV. SUMMARY AND DISCUSSION

This paper has investigated the stochastic process formed by the zeros or stationary points of Gaussian random pro-

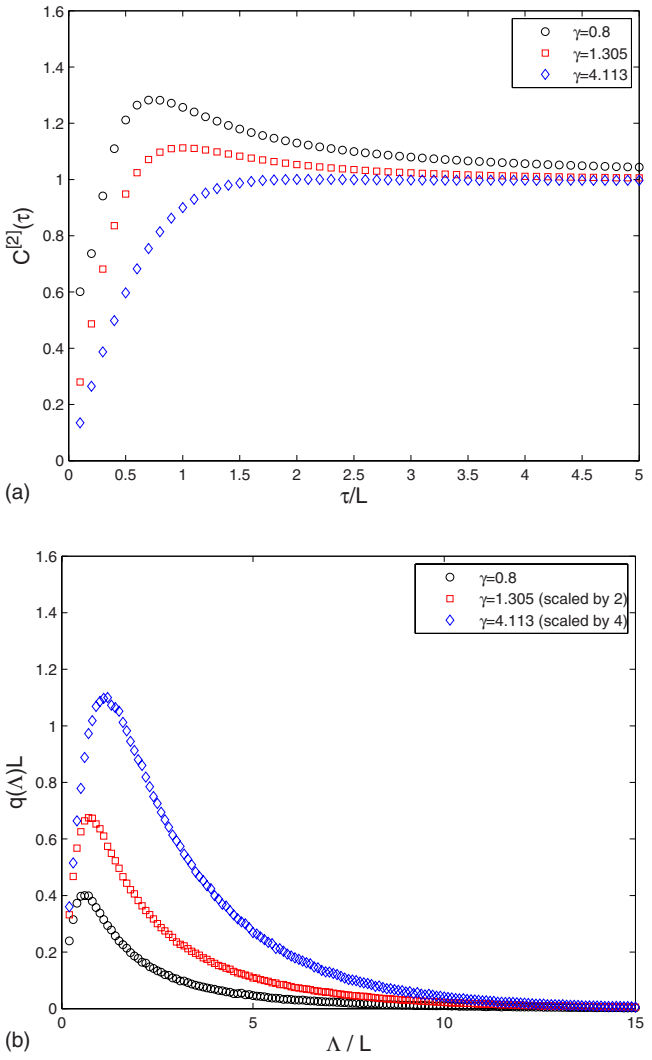

FIG. 7. (Color online) (a) Normalized autocorrelation function $C^{[2]}$ of the zeros of Gaussian processes correlated with ρ_3, plotted as a function of the delay time in correlation lengths τ/L. The circles, squares, and diamonds correspond to values of γ equal to 0.8, 1.305, and 4.113, respectively. In (b), the normalized interevent densities of the zeros of the Gaussian process are shown, where the symbols correspond to the same values of γ as in (a). The densities have been scaled so that they may be distinguished. All figures are simulated with $L=10$ and averaged over 1.5×10^6 realizations.

cesses that are generated from three classes of autocorrelation function. These point processes exhibit a range of behaviors that can be characterized according to their location in the landscape charted by the parameters that affect the autocorrelation function. The results of this paper are summarized in Table I, together with results that pertain to other aspects of this problem that have appeared elsewhere.

This paper has demonstrated that there are three principal qualities that affect the process formed by the zero crossings.

(i) *The Fano factor.* This depends on the global properties of the autocorrelation function of the Gaussian process via Eq. (2) and influences the distribution of the zeros.

(ii) *The smoothness of the underlying Gaussian process.* Whether the process has subfractal characteristics which influence the propensity for the zeros to form into clusters and affects their temporal evolution as manifested in their autocorrelation function and inter event probability densities.

(iii) *The existence of multiple scales of the underlying Gaussian process.* This influences whether the cluster of zeros are themselves clustered which is manifested by oscillations in the autocorrelation function and bimodal interevent probability densities.

We have concentrated on models of autocorrelation function for the Gaussian processes that encapsulate many of the behaviors seen in practice. The statistical behavior of the zeros is affected principally by the structure of the autocorrelation function in the vicinity of the origin. The first model is a two-scale modified Gaussian function that is subfractal when $0<\mu<2$. The parameter b affects the second scale size. The second two-scale model is that for modified LCR noise whose principal differences are that there is always a cubic term in the expansion of the autocorrelation function about the origin and the longer correlation memory that has an exponential rather than Gaussian falloff for large delay times.

The locus for where the second scale size becomes smaller than the outer scale is shown in Fig. 1; above this line the zeros tend to form into bunches whereas below the line the converse is the case. Within any bunch, the zeros form subclusters if $\mu<1$ or are repelled from each other if $\mu>1$, which is a gauge of the smoothness of the Gaussian process.

Notice that any contour for which $F>1$ passes through the antibunching to bunching regimes as μ is increased whereas this is not necessarily the case for some contours with $F<1$. Prominent features in the autocorrelation function of the zeros also appear in the interevent densities. Bunching becomes more prevalent as the neighborhood of the two-scale locus is traversed in the direction of increasing F, the interevent densities broaden and eventually become bimodal, these peaks being characteristic of the intra- and intercluster intervals. This can be contrasted with, for example, the results of [9], where the interevent densities are unimodal precisely because the correlation function considered was appropriate for a perfectly smooth process. For the modified Gaussian and LCR autocorrelation models, which are exponentially bounded, the interevent densities have exponential tails irrespective of whether clustering occurs. The last autocorrelation model considered was for a single scale but with power-law asymptote. No clustering can occur for this model. The autocorrelation function for the zeros decays very slowly in this instance but the asymptotic behavior of the interevent densities remains exponential unless $\gamma<1$, whereupon it becomes a stretched exponential [41,42].

All the processes treated in this paper are at least once differentiable and so possess a degree of "smoothness". This is not true of fractal processes that have autocorrelation function with expansion

$$\rho(\tau) = 1 - a\tau^{2\mu} + \cdots$$

close to the origin. The trace of these objects has an inverse cascade, revealing successively more detail at finer scales but without being resolved through magnification. The zeros

TABLE I. Summary of the behavior of the zeros of Gaussian processes correlated with either fractal, subfractal, or power-law autocorrelation functions. Detail is provided of the distribution of the zeros, their interevent densities, and their autocorrelation functions.

$\rho(\tau)$	$p(N)$	Correlation	$q(\Lambda)$
Fractal $1-a\tau^{2\nu}+\ldots$, $\tau \ll 1$, $0<\nu<1$ $\exp(-\tau)$, $\tau \gg 1$	$F=\infty$ Stable with index ν	Extreme clustering	$\Lambda^{-2+\nu}$, $\Lambda \ll 1$ $\exp(-\Lambda)$, $\Lambda \gg 1$
SubFractal $1-\frac{1}{2}\tau^2+b\tau^{2+\mu}+\cdots$, $\tau \ll 1$, $0<\mu<2$ $\exp(-\tau^q)$, $\tau \gg 1$, $q \geq 1$	$F>1$, Negative binomial $F=1$, Poisson $F<1$, Binomial	Bunched $b>1/2^{2+\mu}$ Antibunched $b<1/2^{2+\mu}$	bimodal, unimodal; $\exp(-\Lambda)$, $\Lambda \gg 1$
Smooth, power-law asymptote $1-1/2\tau^2+b\tau^4+\cdots$, $\tau \ll 1$ $\tau^{-\gamma}$, $\tau \gg 1$	$F>1$, Negative binomial $F=1$, Poisson $F<1$, Binomial	Antibunched	$\exp(-\Lambda)$, $\gamma>1$, $\Lambda \gg 1$ $\exp(-\Lambda^\gamma)$, $\gamma<1$, $\Lambda \gg 1$

group in clusters, there being an infinite number in any cluster. The Fano factor for these processes is infinite and the distribution for the number of zeros has a power-law tail, $p(N) \sim 1/N^{1+\mu}$ [50], which is one of the discrete stable distributions. The interval density for these has a power-law form for small intervals, but retains the exponential tail [51]. Fractal processes therefore display the least complex but most marked departures from the behaviors described in this paper. Their properties are listed in the first row of Table I, in order to complete the picture.

It is surprising, perhaps, that the occurrence of Poisson distributed zeros is the exception rather than the norm, occurring in the μ-b space on the contours where $F=1$. Note however that realizations of these never form a Poisson *process*, which is an uncorrelated series of events with independent, exponentially distributed intervals. This should be contrasted with distributions for the number of extrema or crossings at a high level [38], which have been shown to be asymptotically Poisson distributed. However, this description obscures a more complex behavior, whereby the crossings evolve as pairs of events, and this will be treated fully elsewhere where modifications due to the continuous process being non-Gaussian will also be discussed.

When the interval T is small compared with the characteristic scale length L, the distribution of zeros should ostensibly become binomial since a zero either occurs in a short interval, or does not. However, even though the mean and second moment vanish in this limit, $\langle N(N-1)\rangle$ does not scale as $\langle N\rangle^2$ and so the distribution of zeros cannot be described by a scaling distribution [52]. This implies that the zeros cannot be exactly binomial in this limit, because the binomial distribution *is* an example of a scaling distribution. In the large T limit, all the limiting forms of the distributions of N *are* examples of scaling distributions. Therefore, there is an evolution from nonscaling to scaling distributions as T increases. A determination of the way by which this change occurs would be a fruitful area for further study.

Despite their specificity, the autocorrelation functions adopted in this paper provide sufficiently generic models with which to qualitatively identify and understand the trends that result from more complex situations. For example, the greater the number of distinct scale sizes, the more modulation will occur between the clusters of zeros, leading to a hierarchy of clustering. Within the smallest cluster size, the smoothness of the continuous process dictates whether the zeros are well separated or incipiently bunched. This picture will become clouded if the continuous process is non-Gaussian, for then the higher order correlation properties are not prescribed in terms of the lowest order autocorrelation function alone. Hence the zeros will be affected by a parameter space of higher dimension. Significant modelling and interpretive challenges are presented if the continuous process is nonstationary. Some inroads can be made by assuming stationary increments, enabling models to be constructed for the structure function rather than the autocorrelation function. Further complexity and richness of behaviors will result from a consideration of (Gaussian or otherwise) random fields (e.g. [53] and references therein), where the nature of the stationary points have implications for vector properties of the processes that the fields represent.

ACKNOWLEDGMENTS

J.M.S. acknowledges the support of the EPSRC and Leverhulme Trust. We thank R. O'Dea who assisted in the production of the figures.

APPENDIX

This appendix gives expressions for the power spectra of the three correlation models used. These power spectra must

be positive definite functions and this constrains the values of the parameters that are used in the models for ρ_1 and ρ_2. Because the autocorrelation functions used are real-valued and symmetric, the power spectrum is the Fourier-cosine transform of autocorrelation function:

$$\bar{\rho}(\omega) = 2\int_0^\infty \rho(t)\cos(\omega t)dt$$

These can be evaluated in terms of tabulated functions to give

$$\frac{\bar{\rho}_1(\omega)}{L} = \pi^{1/2}\exp\left[-\left(\frac{L\omega}{2}\right)^2\right] + 2^{(\mu+2)/2}b\Gamma\left(\frac{3+\mu}{2}\right){}_1F_1\left[\frac{3+\mu}{2},\frac{1}{2};-\frac{1}{2}(L\omega)^2\right],$$

where Γ is the gamma function [54] and ${}_1F_1$ the confluent hypergeometric function [55],

$$\frac{\bar{\rho}_2[\omega]}{L} = 2[1+(L\omega)^2]^{-2} + b\Gamma(3+\mu)[1+(L\omega)^2]^{-(3+\mu)/2} \times\cos[(3+\mu)\arctan(L|\omega|)]$$

and if $b<0$ there is always some value of ω for which these two power spectra are negative, as can be readily verified using graphical methods. By contrast,

$$\frac{\bar{\rho}_3(\omega)}{L} = \frac{2^{(3-\gamma)/2}\pi^{1/2}\gamma^{(\gamma+1)/4}}{\Gamma(\gamma/2)}(L|\omega|)^{(\gamma-1)/2}K_{(\gamma-1)/2}(L|\omega|\gamma^{1/2}),$$

where K_ν is a modified Bessel function [55], and this function is positive definite for all values of its parameters.

[1] D. Poland, Biophys. Chem. **110**, 59 (2004).
[2] A. I. Kostyukov, Y. N. Ivanov, and M. V. Kryzhanovsky, Biol. Cybern. **39**, 157 (1981).
[3] M. Schindler, P. Talkner, and P. Hanggi, Phys. Rev. Lett. **93**, 048102 (2004).
[4] D. Middleton, *An Introduction to Statistical Communication Theory* (McGraw-Hill, New York, 1960).
[5] R. Wiley, IEEE Trans. Commun. **29**, 1061 (1981).
[6] I. Rychlik, P. Johannesson, and M. R. Leadbetter, Mar. Struct. **10**, 13 (1997).
[7] M. Constantin and S. Das Sarma, Phys. Rev. E **72**, 051106 (2005).
[8] M. C. Wu, M. C. Huang, H. C. Yu, and T. C. Chiang, Phys. Rev. E **73**, 016118 (2006).
[9] B. Derrida, V. Hakim, and R. Zeitak, Phys. Rev. Lett. **77**, 2871 (1996).
[10] S. N. Majumdar, C. Sire, A. J. Bray, and S. J. Cornell, Phys. Rev. Lett. **77**, 2867 (1996).
[11] S. N. Majumdar and C. Sire, Phys. Rev. Lett. **77**, 1420 (1996).
[12] A. Dhar and S. N. Majumdar, Phys. Rev. E **59**, 6413 (1999).
[13] V. A. Ivanov, Theor. Probab. Appl. **5**, 319 (1960).
[14] H. Cramer and M. R. Leadbetter, *Stationary and Related Stochastic Processes* (Wiley, New York, 1967).
[15] T. L. Malevich, Theor. Probab. Appl. **14**, 287 (1969).
[16] G. Lindgren, Adv. Appl. Probab. **4**, 81 (1972).
[17] M. R. Leadbetter, in *Stochastic Point Processes*, edited by P. A. W. Lewis (Wiley-Interscience, New York, 1972).
[18] I. F. Blake and W. C. Lindsey, IEEE Trans. Inf. Theory **19**, 295 (1973).
[19] J. Abrahams, in *Communications and Networks*, edited by F. Blake and H. V. Poor (Springer-Verlag, New York, 1986).
[20] E. Jakeman and D. T. J. Hurle, Phys. Fluids **16**, 2056 (1973).
[21] C. Koch, *Biophysics of Computation: Information Processing in Single Neurons* (Oxford, New York, 1999).
[22] J. C. Eccles, *The Physiology of Nerve Cells* (John Hopkins University Press, Baltimore, 1957).
[23] K. Christensen, A. Corral, V. Frette, J. Feder, and T. Jossang, Phys. Rev. Lett. **77**, 107 (1996).
[24] K. I. Hopcraft, E. Jakeman, and R. M. J. Tanner, Phys. Rev. E **64**, 016116 (2001).
[25] F. Lillo and R. N. Mantegna, Phys. Rev. E **68**, 016119 (2003).
[26] N. Menyhard and G. Odor, Phys. Rev. E **68**, 056106 (2003).
[27] G. Blum, S. Gnutzmann, and U. Smilansky, Phys. Rev. Lett. **88**, 114101 (2002).
[28] S. O. Rice, Bell Syst. Tech. J. **23**, 282 (1944).
[29] M. Kac, Bull. Am. Math. Soc. **49**, 314 (1943).
[30] E. V. Bulinskaya, Theor. Probab. Appl. **6**, 435 (1961).
[31] N. D. Ylvisaker, Ann. Math. Stat. **36**, 1043 (1965).
[32] J. T. Barnett and B. Kedem, IEEE Trans. Inf. Theory **37**, 1188 (1991).
[33] M. R. Leadbetter and G. V. Spaniolo, Statistica Neerlandica **56**, 152 (2002).
[34] K. Sharpe, Adv. Appl. Probab. **10**, 373 (1978).
[35] R. Barakat, J. Opt. Soc. Am. A **5**, 1244 (1988).
[36] H. Steinberg, P. M. Schultheiss, C. A. Wogrin, and F. Zweig, J. Appl. Phys. **26**, 195 (1955).
[37] R. N. Miroshin, Vestn. St. Petersburg Univ. Math. **34**, 30 (2001).
[38] H. Cramer, Theor. Probab. Appl. **10**, 126 (1965).
[39] U. Fano, Phys. Rev. **72**, 26 (1947).
[40] E. Wong, SIAM J. Appl. Math. **14**, 1246 (1966).
[41] J. F. Eichner, J. W. Kantelhardt, A. Bunde, and S. Havlin, Phys. Rev. E **75**, 011128 (2007).
[42] P. Olla, Phys. Rev. E **76**, 011122 (2007).
[43] G. F. Newell and M. Rosenblatt, Ann. Math. Stat. **33**, 1306 (1962).
[44] E. Jakeman, Opt. Acta **28**, 435 (1981).
[45] M. V. Berry, J. Phys. A **12**, 781 (1979).
[46] S. B. Lowen and M. C. Teich, *Fractal-based Point Processes* (Wiley Interscience, New York, 2005).
[47] W. B. Davenport and W. L. Root, *An Introduction to the Theory of Random Signals and Noise* (IEEE Press, New York,

1987).
[48] E. Jakeman and K. D. Ridley, *Modeling Fluctuations in Scattered Waves* (Taylor and Francis, New York, 2006).
[49] D. B. Percival, Comp. Sci. Stat. **24**, 534 (1992).
[50] K. I. Hopcraft, P. C. Ingrey, and E. Jakeman, Phys. Rev. E **76**, 031134 (2007).
[51] J. O. Matthews, K. I. Hopcraft, and E. Jakeman, J. Phys. A **36**, 11585 (2003).
[52] F. Ghielmetti, Nuovo Cimento Soc. Ital. Fis., B **35**, 243 (1976).
[53] I. Freund, J. Opt. Soc. Am. A **15**, 1608 (1998).
[54] I. S. Gradshteyn and I. M. Ryzhik, *Table of Integrals, Series, and Products*, 5th ed. (Academic Press, London, 1994).
[55] M. Abramowitz and A. Stegun, *Handbook of Mathematical Functions*, 9th ed. (Dover, New York, 1970).